

Thermal Behavior of Aqueous Solutions of Hydroxylamine During Isothermal and Iso-peribolic Decomposition in a Closed System[†]

Maria I. Papadaki* and Eleni Pontiki

Department of Environmental and Natural Resources Management, University of Ioannina, Agrinio GR30100, Greece

Lijun Liu, William J. Rogers, and M. Sam Mannan

Mary Kay O'Connor Process Safety Center, Artie McFerrin Department of Chemical Engineering, Texas A&M University, College Station, Texas 77843-3122

Hydroxylamine (HA) has been independently involved in several tragic accidents, which incurred numerous fatalities and injuries. Following these incidents, adiabatic calorimetry and computational chemistry research was conducted, suggesting potential reaction pathways of HA decomposition, but the mechanism of HA behavior still has not been completely understood. In the present work, the thermal decomposition of hydroxylamine was studied via isothermal and isoperibolic calorimetric measurements in a glass and in a metal reactor, respectively. Identification of stable intermediates, like ammonia, nitrates, or nitrites during the course of the reaction did not provide any conclusive results. The calorimetric measurements presented here show condition-dependent endothermic and exothermic reaction steps that are consistent with previous findings of computational chemistry. These findings corroborate previously reported results, according to which the NH_2^- moiety may trigger reaction runaway.

Introduction

Hydroxylamine (HA) is widely used as a flaking-off agent and a metallic surface treatment agent in the semiconductor¹ and pharmaceutical industries.² Hydroxylamine and its salts are extensively used as a reducing agent in numerous organic and inorganic reactions, for example.^{3–6} They can also act as antioxidants for fatty acids. HA has also been used in the past by biologists to introduce random mutations. Some nonchemical uses include removal of hair from animal hides and photography developing solutions.⁷ The nitrate salt, hydroxylammonium nitrate, is being researched as a rocket propellant, in water solution as a monopropellant, and in its solid form as a solid propellant.^{8,9}

HA may explode on heating above 343 K or when exposed to open flame. The substance decomposes rapidly at room temperature, especially in the presence of moisture and carbon dioxide, and violently on heating, producing toxic fumes including nitrogen oxides. The solution in water is a weak base.⁹ The thermal instability of hydroxylamine is reduced in aqueous solutions. The maximum mass fraction of hydroxylamine in water is 0.5 in commercial grade.¹⁰

HA is moderately toxic to man, animals, and even plants. Acute as well as chronic exposure has been shown to be hemotoxic. It has been shown to be an inhibitor of enzymes and viruses. It is a strong mutagen¹¹ with reported activity against phages, viruses, bacteria, fungi, protozoa, *Drosophila*, and plants.¹²

Since 1999, hydroxylamine (HA) has been involved in two tragic accidents,^{13–15} which incurred numerous fatalities and injuries. Following these two incidents, extensive research on

hydroxylamine thermal decomposition has been conducted.^{1,16–25} Previous research at the Mary Kay O'Connor Process Safety Center in the Chemical Engineering Department at Texas A&M University had focused on adiabatic calorimetry tests, which have provided the temperature, pressure, and heat generation history of hydroxylamine decomposition under selected runaway conditions. Quantum chemistry calculations have also been employed to elucidate the elementary reactions occurring during its thermal decomposition.^{25,26} Finally, based on the decomposition end products, the most likely of the potential reaction paths had been identified.^{22,25}

The research presented here is part of a long-term project, which aims to develop a generalized methodology for the identification of reaction pathways, kinetics, and measurement of reaction enthalpy, of rapid, condition dependent thermal decomposition reactions, where hydroxylamine is employed as a typical model compound. The thermal behavior of such reactions is traditionally studied via differential scanning calorimetry and different forms of adiabatic calorimetry (DSC-AC), a detailed description of which can be found elsewhere.^{27–33} However, these techniques do not provide reliable data for extrapolation of condition-dependent decomposition reactions.

Hydroxylamine thermal decomposition proceeds via a complex reaction-network of short-life intermediates the formation/destruction of which is condition-dependent.^{18,19,21,22} Because of its thermal instability and the high pressures produced by its decomposition, the experimental amounts of hydroxylamine must be small and the employed sample cells relatively small, too. These restrictions however impose further limitations on the potential analytical techniques that can be employed for the identification and quantification of unstable and even some stable intermediates. The simultaneous identification and quantification of coexisting ammonia, nitrates, nitrites and other nitrogen

[†] Part of the "William A. Wakeham Festschrift".

* To whom correspondence should be addressed. E-mail: mpapadak@cc.uoi.gr; m.papadaki@leeds.ac.uk. Tel: +30 26410 74184. Fax: +30 26410 74176.

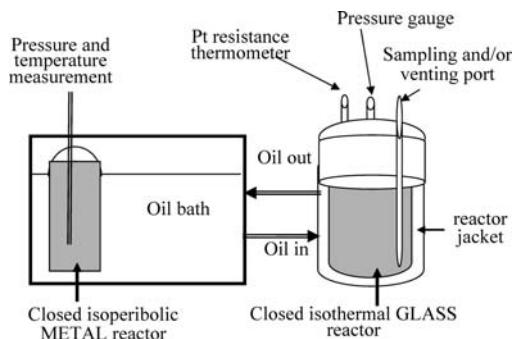


Figure 1. Isothermal and isoperibolic reactor arrangement.

containing moieties is difficult,³⁵ especially when only small samples can be used, which inevitably limit the potential use of different analytical techniques. So far, collected evidence indicates that computational chemistry is an effective tool for this work. However, the generation of reliable computational results requires a firm experimental backing.

Experimental Section

Materials and Methods. Hydroxylamine isothermal decomposition measurements were performed in the temperature range of (373.15 to 425.15) K using an HEL SIMULAR isothermal calorimeter³⁶ operated in the isothermal and/or isoperibolic mode. Figure 1 shows the employed reactor arrangement. An in-house made pressure-resistant glass jacketed reactor with a liquid holding capacity of (120 ± 2) cm³ and a total volume of (250 ± 2) cm³ was used (glass reactor 2 in Figure 1). Glass reactor temperature was measured by small platinum resistance thermometers (accuracy better than 0.5 K) and the bath temperature was controlled by the SIMULAR unit to remain constant at the desired temperature by means of the thermal oil circulated in the reactor jacket. The bath oil temperature variations were small, so a second high-pressure metal reactor of a total capacity of (40 ± 1) cm³ was submerged in the oil bath for the isoperibolic measurements. Liquid samples of less than 0.5 cm³ were regularly withdrawn from the glass reactor to be further analyzed via UV, high performance liquid chromatography (HPLC), and ion chromatography (IC). When glass and metal reactors were employed simultaneously, the same initial composition reacting mixtures were used in both reactors. The metal reactor was inserted in the bath when its temperature, measured by a regularly tested and calibrated type N thermocouple, with accuracy better than (± 1) K, had reached approximately 373 K. The bath temperature was the one dictated by the isothermal glass reactor control system. (A typical temperature profile for such a measurement is shown in Figure 4.) Pressure was measured with Omega Eng. Inc. pressure gauge 2.068 MPa full scale with a precision of (± 0.0172) MPa.

For purely isoperibolic measurements, the bath temperature was maintained at the stated temperature with an accuracy of (± 0.2) K. Isoperibolic measurements were performed in the metal and isothermal in the glass reactor. No samples were taken from the metal reactor. Only its end products were analyzed.

Products were analyzed via HPLC, and IC (not shown here). HPLC measurements were performed using a Dionex P680 system with a Dionex 1024 dio-array equipped with an Acclaim C18 5 μ m 120 Å, 406 mm \times 250 mm column using a 95:5 water/acetonitrile isocratic mobile phase at 1 cm³ min⁻¹ with UV detection at 201 nm, 206 nm, 210 nm, 530 nm or 220 nm, and 254 nm. IC measurements employed a Dionex ICS 1500 chromatograph with a 9 mM sodium carbonate mobile phase.

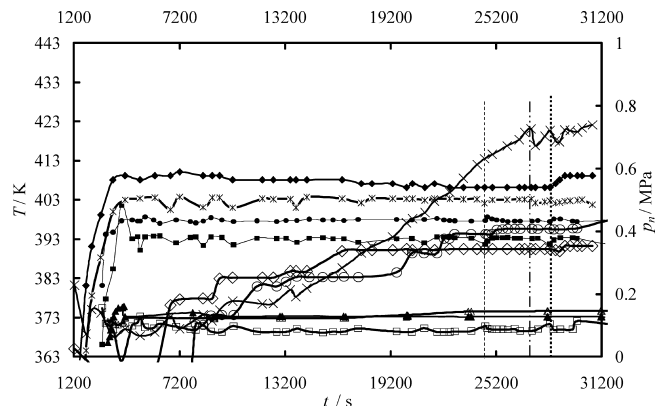


Figure 2. Normalized pressure, p_n , and temperature, T , profiles, as a function of time, t , of isothermal measurements in glass reactor [G(1) to G(3) with temperature control set for isothermal glass reactor operation, as shown in Table 1] and isoperibolic measurements in metal reactor [M(2) and M(3) with temperature control set for isothermal glass reactor operation, as shown in Table 1]. Temperatures are read on the left-hand axis and pressures on the right-hand axis. \blacktriangle , glass reactor temperature of measurement G(1) and \triangle , its pressure. \blacksquare , glass reactor temperature of measurement G(2) and \square , its pressure. \bullet , metal reactor temperature of measurement M(2) and \circ , its pressure. $*$, glass reactor temperature of measurement G(3) and \times , its pressure. \blacklozenge , metal reactor temperature of measurement M(3) and \diamond , its pressure.

Hydroxylamine was supplied by Fluka in a aqueous solution. Hydroxylamine mass fraction was 0.5 (product code 55458 purum) and was used without further purification. Milli-q water was used for all dilutions.

Results and Discussion

Figure 2 shows the pressure and temperature history of three isothermal (in glass reactor) and two isoperibolic (in metal reactor) measurements. Quantities of hydroxylamine and water employed in each measurement and temperature control information are provided in Table 1. Given masses were weighed with a precision better than ± 0.01 g. The pressure and temperature history of isoperibolic measurements M(2) and M(3) of Table 1, at 397.15 K and 409.15 K, respectively, are shown in Figure 2. They were taken with both reactors operating simultaneously. Temperatures (most indicated with closed markers) are read on the left-hand ordinate. Absolute (normalized) pressures (indicated with open markers) are read on the right-hand ordinate. Markers of the same shape correspond to the same measurement. The reactor temperature in isothermal measurements and the steady-state metal reactor temperature (obtained after reaction completion) in isoperibolic ones are shown in the first column of Table 1. For comparison purposes, the pressures measured were normalized to the temperature of 409.15 K and the volume of 90 cm³, according to relation (1), assuming ideal gas behavior.

$$(p_n/\text{MPa}) =$$

$$(p/\text{MPa} - p^0/\text{MPa}) \cdot [(407.15 \text{ K}) / (T/\text{K})] + (V/90 \text{ cm}^3) \quad (1)$$

where p_n is the absolute normalized pressure, p is the measured absolute pressure, T is the mixture absolute temperature, p^0 is the vapor pressure of water at temperature T , and V is the mixture volume in cm³. The vapor pressure of hydroxylamine or the thermal expansion of the liquid have not been taken into account. However, as this work focuses on qualitative results, this approach is not expected to change any qualitative conclusions.

It can be seen in Figure 2, that as expected, isothermal measurement temperatures are a few degrees lower than the

Table 1. Hydroxylamine and Water Mass in Reported Experiments^a

measurement	reference temperature	HA	H ₂ O	total	reactor type and measurement code	temperature control mode and set-point
	<i>T</i> /K	<i>m</i> /g	<i>m</i> /g	<i>m</i> /g		
373.15	373.15	25.77	80.00	105.77	G(1)	isothermal at 373.15 K
397.15	397.15	4.87	15.13	20.00	M(2)	isothermal at 397.15 K
393.15	393.15	30.22	93.85	124.07	G(2)	isothermal at 393.15 K
409.15	409.15	2.23	7.77	10.00	M(3)	isothermal at 409.15 K
403.15	403.15	13.10	45.60	58.70	G(3)	isothermal at 403.15 K
413.15	413.15	2.81	7.61	10.42	M(4)	isoperibolic at 413.15 K
414.15	414.15	2.85	7.90	10.75	M(5)	isoperibolic at 421.15 K
425.15	425.15	2.73	7.86	10.59	M(6)	isoperibolic at 433.15 K

^a Reactor type is indicated as G for glass reactor and M for metal reactor. Measurements are indicated as (1), (2), etc. In measurements (1), (2), and (3), temperature control was set to maintain isothermal glass reactor operation. Measurement reference temperature indicates the reactor steady-state temperature. Temperature was controlled so as either to maintain constant temperature at the glass reactor, indicated in the last column as "isothermal" or so as to maintain constant circulator temperature indicated here as "isoperibolic". The temperature set-point of each measurement is shown in the same column.

isoperibolic ones, when the two reactors were operated simultaneously. From calorimetric data, there is no evidence of HA decomposition in the glass reactor measurement G(1), at 373.15 K (triangular markers), or G(2) at 393.15 K (square markers), during the approximately $32 \cdot 10^3$ s of the measurement, as no pressure rise appears. However, as reported in our previous work,¹⁶ HPLC analyses showed that reactions, which do not produce any noncondensable gases, do occur. The observed temperature and pressure undulations were due to sampling. No temperature change is apparent for measurement M(2) in the metal reactor (closed circular markers) at 397 K; however, the reactor pressure started rising after $8.5 \cdot 10^3$ s, thus indicating reaction in progress. Although M(2) measurement temperature is a few degrees higher than that of measurement G(2), catalysis effects^{1,21} and not temperature are more likely to be responsible for the manifestation of the reaction via a pressure rise. The pressure leveled off at 0.4 MPa.

In measurement G(3), at 403.15 K (star markers), pressure starts rising at approximately $7.8 \cdot 10^3$ s. The pressure rise profile was not smooth. After $12 \cdot 10^3$ s, the glass reactor pressure started rising steadily and at $24 \cdot 10^3$ s it was approaching the maximum operational pressure of the glass reactor. At approximately $24.6 \cdot 10^3$ s, indicated here with a dashed vertical line, to prevent the glass reactor from breaking, some liquid from the reactor was removed. However, no pressure drop was observed; on the contrary, the reactor pressure shortly started rising further. It was thus decided to proceed with some further removal of the liquid reacting mass, $2.4 \cdot 10^3$ s later (also shown in the figure with a vertical line) followed by a subsequent liquid mass discharge $1.2 \cdot 10^3$ s later (shown in the figure as a vertical dotted line).

Immediately after the liquid removal at $24.6 \cdot 10^3$ s, there was a significant temperature rise of the oil leaving the reactor, (shown later in Figure 5), which continued increasing following the subsequent liquid discharges, potentially also affecting the temperature of the isoperibolic reactor, as can be seen in the closed diamond curve of the metal reactor temperature. Shortly after the last discharge the glass reactor broke.

The normalized absolute pressure (p_n) and the temperature profiles of the isothermal measurement G(3) in the glass reactor at 403.15 K, where regular sampling was taking place and the simultaneous isoperibolic run in the closed-system metal reactor, M(3), at 409.15 K can be seen more clearly in Figure 3, where arrows pointing at the pressure curve, indicate sampling.

As can be seen in Figure 3, the normalized absolute pressure of the metal reactor where no sampling or removal of mass took place was rising gradually maintaining long periods of constant pressure. It can be also seen that the temperature of the same reactor drops while the pressure is

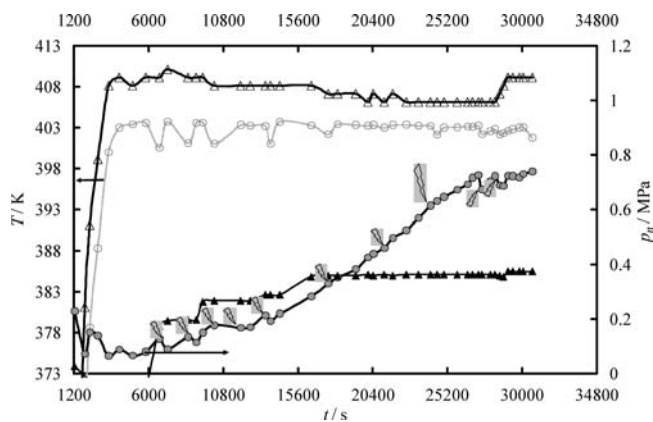


Figure 3. Normalized pressure, p_n , (according to eq 1) and temperature profile, T , of isothermal glass reactor measurement G(3) and isoperibolic metal reactor measurement M(3) (with temperature control set for isothermal glass reactor operation at approximately 403 K, as shown in Table 1), as a function of measurement time, t . Δ , metal reactor temperature of measurement M(3) and \blacktriangle , its normalized pressure. \circ , glass reactor temperature of measurement G(3) and gray-filled circle, its normalized pressure. Arrows indicate selected sampling/venting points.

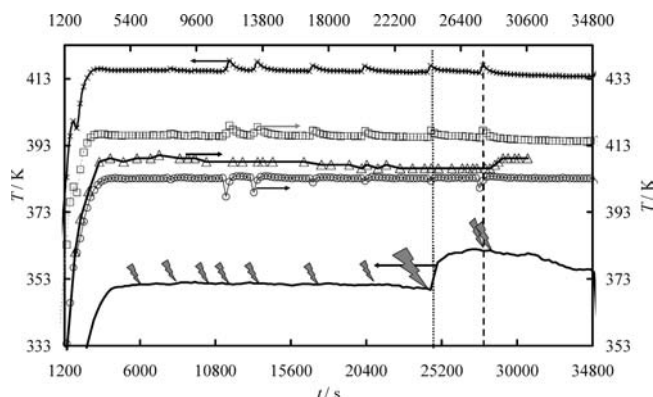


Figure 4. Temperature, T , versus time, t , profiles. Glass and metal reactor temperature history, temperature history of oil entering and leaving the glass reactor and oil bath temperature as a function of time of joined isothermal and isoperibolic measurements G(3) and M(3), respectively, shown in Table 1. From top to bottom: \times , oil in temperature; \square , circulator temperature; Δ , metal reactor temperature; \circ , glass reactor temperature; and $- \cdot -$, oil leaving the glass reactor. Arrows in the oil leaving the glass reactor curve show approximate sampling/venting times.

constant, indicating an endothermic reaction taking place. The final pressure of this reactor at approximately $32 \cdot 10^3$ s was roughly the same as the final pressure of measurement M(2), where more than the double amount of hydroxylamine was used, thus indicating that hydroxylamine decomposition

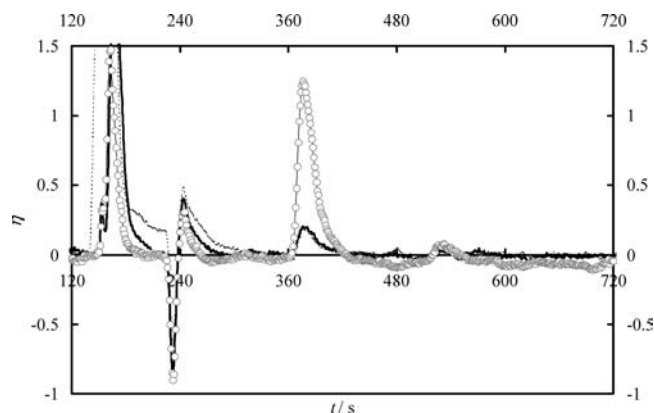


Figure 5. UV absorbance, α , at 254 nm during HPLC analyses of different samples, taken from the glass reactor during measurement G(3) (as shown in Table 1), as a function of retention time, t . Arrows in the oil leaving the reactor curve of Figure 4 show the sampling time-sequence. —, seventh sample taken at approximately $21 \cdot 10^3$ s, \circ , eighth (large) sample taken at approximately $24 \cdot 10^3$ s, and - - -, ninth sample taken at $27.5 \cdot 10^3$ s.

at 397.15 K in the metal reactor, measurement M(2), had not reached completion. On the other hand, the normalized absolute pressure of the glass reactor was constantly rising. In our previous work,¹⁶ it was shown that no calorimetric evidence of reaction (i.e., no pressure or temperature rise) was observed in isothermal measurements of HA aqueous solutions in a closed glass-cell at 403.15 K performed in the adiabatic pressure tracking calorimeter for a period over $66 \cdot 10^3$ s. It is thus plausible that it was sampling that caused a rapid generation of noncondensable gases, thus increasing the glass reactor pressure. HPLC analyses of the final products showed that hydroxylamine in measurement M(3) had reacted fully in the metal reactor, where catalysis effects were expected to accelerate the reaction,^{1,21} although in the glass reactor, despite the inevitable loss of reacting mass during venting, the reaction had not reached completion. HPLC analysis showed that hydroxylamine in measurement M(2) had also not reacted fully.

Figure 4, shows the temperature of the oil entering and leaving the glass reactor, the circulator temperature and the temperatures of the glass and metal reactors. In order to reduce curve congestion in the figure, both ordinates have been used to represent the temperatures, but the temperature ranges shown are of equal length, so easier comparisons can be made. All sampling sequence has been marked on the oil leaving the glass reactor curve, but it can be indirectly seen in the remaining curves, as sampling affects glass reactor, oil entering the glass reactor, jacket, and circulator temperatures. However, in most cases the temperature of the oil leaving the glass reactor manifests better the changes occurring in the reactor.

As the oil leaving the glass reactor jacket indicates, a significant temperature rise occurred in the glass reactor at $24.6 \cdot 10^3$ s, and the higher temperature reached was maintained until the reactor broke. Moreover, as shown in Figure 4, the lower temperature of the metal reactor shortly before the end of the experiment cannot be justified by any drop of the circulator temperature.

In our previous work,¹⁶ we reported an unknown compound, potentially the NH_2^- moiety, quantified at 254 nm with a retention time of 384 s, as a suspect factor that triggers the reaction runaway. The current measurements provide further support to this assumption. Figure 5 shows the UV absorption factor, α , at 254 nm from the HPLC analysis of

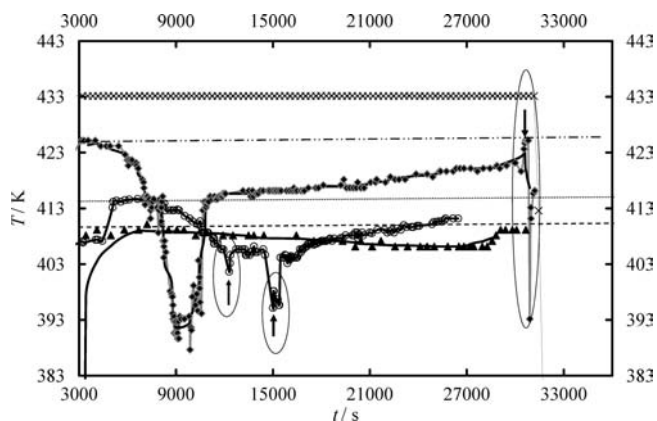


Figure 6. Temperature, T , profiles, as a function of time, t , of isoperibolic measurements M(3), M(5), and M(6) (shown in Table 1) with and without venting. Arrows indicate points of venting. \blacktriangle , temperature of measurement M(3) taken with control at isothermal glass reactor at 403.15 K, as indicated in Table 1. \circ , temperature of measurement M(5) taken at constant bath-temperature at 421.15 K, as indicated in Table 1. \blacklozenge , metal reactor temperature and \times , circulator temperature of measurement M(6) taken at constant bath temperature at 433.15 K, as indicated in Table 1. Different forms of dotted lines show the reference temperature of each isoperibolic measurement.

typical samples obtained during this measurement. As can be seen in Figure 5, the eighth sample, obtained just before the sudden rise of the oil leaving the glass reactor temperature, shows this compound at a much higher concentration than the one encountered in its previous and next to it samples. The concentration of this compound in the first and the last samples was much smaller than the ones shown here. Although adiabatic measurements of hydroxylamine thermal decomposition have been reported to be unaffected by the presence of air,²² it cannot be ruled out that the larger amount of oxygen available in the experiment performed in the glass reactor, compared to the oxygen that was present in the smaller metal reactor container or in the cell employed by Cinseros et al.,²² contributed to the reaction runaway. Similarly, in measurement M(2) where reaction did not reach completion, the temperature was lower but oxygen availability was also much less than the one in measurement M(3), as the liquid-reacting mixture occupied much more of the reactor space. Oxidation of hydroxylamine³⁷ may have played a role.

The effect of reactor venting/liquid discharge was therefore examined, employing the metal reactor only, in isoperibolic measurements. Moreover, the collection of more evidence for potential endothermic reaction was examined.

Figure 6 shows the preliminary results of this investigation. In Figure 6, the temperature history of three measurements M(3), M(5), and M(6) is shown. Measurement M(3), shown with triangular markers, is the temperature profile of the metal reactor temperature, shown previously in Figures 3 and 4. In this measurement, the bath temperature was adjusted in order to maintain the glass reactor temperature constant at 403.15 K. The bath (circulator) temperature stability for this measurement can be seen in Figure 4. As can be seen in Figure 4, bath temperature was disturbed by sampling, although it was maintained constant in the intermediate periods. No reactor venting was applied in this measurement.

Measurements indicated as M(5) and M(6) were performed with the circulator temperature controlled to be constant at (421.15 and 433.15) K, respectively. The (circulator) temperature for measurement M(6) is shown in Figure 6. Circulator temperature stability was similar in measurement

M(5). Although the bath temperature was maintained constant, depending on the reaction temperature, a smoother (for lower bath temperatures) or steeper (for higher bath temperatures) drop in the reactor temperature was observed, clearly indicating an endothermic reaction. No glass reactor measurement or control was implemented here, and the temperature stability of the circulator throughout measurements M(5) and M(6) was better than ± 0.2 K. During the latter two measurements, gas was vented from the reactor as indicated in the figure by the arrows. So, venting took place for the measurement performed at 421.15 K on two occasions, when the temperature started dropping fast at approximately $12 \cdot 10^3$ s and again on the second occasion of the fast temperature drop at approximately $15.6 \cdot 10^3$ s, shown with arrows in Figure 6. The measurement M(6), performed at 433.15 K bath temperature, was vented (removal of gas and vapors) only once at approximately $30 \cdot 10^3$ s. It can be seen that in all cases there was a sharp increase of temperature following reactor venting. In fact, in all cases the rise in temperature was observed the very moment venting initiated.

As can be seen in Figure 6, the temperature drop has a later onset and proceeds more slowly at lower reaction temperatures. This behavior is consistent with that of an endothermic reaction, where the increased temperature affects the reaction rate so that it advances faster, but because of its endothermicity, the temperature drop is also steeper. Because of the reacting mass loss during the venting, no firm quantitative results can be obtained.

As reactor venting provoked sharp temperature rise in the case of isoperibolic reactor and a steep pressure rise in the case of the glass reactor, it is plausible that an intermediate reaction equilibrium is affected by venting, resulting in a fast exothermic, gas-generating reaction path. The above findings are consistent with independent results of computational chemistry.²⁶ However, to our knowledge no such results have been previously reported by other experimental studies. It is however plausible that the powerful heaters employed in adiabatic calorimeters have concealed such a behavior.

Conclusions

Isothermal and isoperibolic decomposition tests were performed on HA aqueous solutions in the temperature range (373.15 to 425.15) K. The research indicates that endothermic reaction steps are involved, which potentially approach a very slow equilibrium with produced gases. Reactor venting drives very fast exothermic steps. Our previous findings of condition dependent autocatalytic decompositions¹⁶ are consistent with those findings. Further experimental work is currently underway targeting first the complete identification of products and stable radicals produced during the decomposition and subsequently the measurement of the heat of reaction during isothermal decomposition.

Acknowledgment

M.P. is indebted to Mary Kay O'Connor Process Safety Center and Chemical Engineering Department, Texas A&M for hosting her for two months while part of the current research was conducted.

Literature Cited

- Iwata, Y.; Koseki, H. Decomposition of Hydroxylamine/Water Solution With Added Iron Ion. *J. Hazard. Mater.* **2003**, *104*, 39–49.
- Cisneros, L. O.; Rogers, W. J.; Mannan, M. S. Adiabatic Calorimetric Decomposition Studies, of 50 wt. % Hydroxylamine/Water. *J. Hazard. Mater.* **2001**, *A82*, 13–24.
- Moffat, K. A.; Hamer, G. K.; Georges, M. K. Stable Free Radical Polymerization Process: Kinetic and Mechanistic Study of the Thermal Decomposition of MB-TMP Monitored by NMR and ESR Spectroscopy. *Macromolecules* **1999**, *32*, 1004–1012.
- Huang, W.; Chiarelli, R.; Charleux, B.; Rassat, A.; Vairon, J. P. Unique Behavior of Nitroxide Biradicals in the Controlled Radical Polymerization of Styrene. *Macromolecules* **2002**, *35*, 2305–2317.
- Manivannan, V.; Goodenough, J. B. Low-Temperature Synthesis of Rutile VO_2 in Aqueous Solution Using $\text{NH}_2\text{OH}\cdot\text{HCl}$ as Reducing Agent. *Mater. Res. Bull.* **1998**, *33*, 1353–1357.
- Cakic, S.; Lacnjevac, C.; Nikolic, G.; Stamenkovic, J.; Rajkovic, M. B.; Gligoric, M.; Barac, M. Spectroscopic Characteristics of Highly Selective Manganese Catalysis in Aqueous Polyurethane Systems. *Sensors* **2006**, *6*, 1708–1720.
- Hydroxylamine. Wikipedia, the free encyclopedia [Online]; Wikimedia Foundation, Posted February 26, 2009. <http://en.wikipedia.org/wiki/Hydroxylamine#Uses> (accessed March 24, 2009).
- Harlow, D. G.; Felt, R. D.; Agnew, S.; Mc Kibben, J. M.; Garber, R.; Lewi, M. Technical Report on Hydroxylamine Nitrate [Online]; U.S. Department of Energy, 1998; pp 2–3. http://www.hss.energy.gov/healthsafety/wshp/chem_safety/docs/hydroxylamine.pdf (accessed March 17, 2009).
- Hydroxylamine. International Chemical Safety Card [Online]; WHO/IPCS/ILO CDC/NIOSH, Posted October 27, 1995 <http://www.cdc.gov/niosh/ipcsneng/neng0661.html> (accessed Jan 28, 2009).
- Standard Interpretations. PSM applicability to a 50% Solution of Hydroxylamine [Online]; USA Department of Labor, OSHA. Posted April 30, 1999. http://www.osha.gov/pls/oshaweb/owadisp.show_document?p_table=INTERPRETATIONS&p_id=22736# (accessed March 24, 2009).
- Budowsky, E. I.; Sverdlov, E. D.; Spasokutskaya, T. A.; Koudelkab, J. Mechanism of the Mutagenic Action of Hydroxylamine: VIII. Functional Properties of the Modified Adenosine Residues. *Biochim. Biophys. Acta* **1975**, *390*, 1–13.
- Gross, P.; Smith, R. P. Biologic Activity of Hydroxylamine: A Review. *Crit. Rev. Toxicol.* **1985**, *14*, 87–99.
- Long, L. A. The Explosion at Concept Sciences: Hazard of Hydroxylamine. *Process Saf. Prog.* **2004**, *23*, 114–120.
- Business Concentrates. Chemical Explosion in Japan Kills Four. *Chem. Eng. News* **2000**, *78* (25), 15–16.
- Reisch, M. Chemical Plant Blast Kills Five Near Alletown. *Chem. Eng. News* **1999**, *77* (9), 11–13.
- Liu, L.; Papadaki, M.; Pontiki, E.; Stathi, P.; Rogers, W. J.; Mannan, M. S. Isothermal Decomposition of Hydroxylamine and Hydroxylamine Nitrate in Aqueous Solutions in the Temperature Range 80–160 °C. *J. Hazard. Mater.* **2009**, *165*, 573–578.
- Liu, Y. S.; Ugaz, V. M.; Rogers, W. J.; Mannan, M. S.; Saraf, S. R. Development of an Advanced Nanocalorimetry System for Material Characterization. *J. Loss Prev. Process Ind.* **2005**, *18*, 139–144.
- Cisneros, L. O.; Rogers, W. J.; Mannan, M. S. Adiabatic Calorimetric Decomposition Studies of 35 Mass % Hydroxylamine Hydrochloride/Water. *Can. J. Chem. Eng.* **2004**, *82*, 1307–1312.
- Wei, C. Y.; Saraf, S. R.; Rogers, W. J.; Mannan, M. S. Thermal Runaway Reaction Hazards and Mechanisms of Hydroxylamine with Acid/Base Contaminants. *Thermochim. Acta* **2004**, *421*, 1–9.
- Cisneros, L. O.; Rogers, W. J.; Mannan, M. S. Comparison of the Thermal Decomposition Behavior for Members of the Hydroxylamine Family. *Thermochim. Acta* **2004**, *414*, 177–183.
- Cisneros, L. O.; Rogers, W. J.; Mannan, M. S.; Li, X. R.; Koseki, H. Effect of Iron Ion in the Thermal Decomposition of 50 Mass % Hydroxylamine/Water Solutions. *J. Chem. Eng. Data* **2003**, *48*, 1164–1169.
- Cisneros, L. O.; Rogers, W. J.; Mannan, M. S. Effect of Air in the Thermal Decomposition of 50 Mass % Hydroxylamine/Water. *J. Hazard. Mater.* **2002**, *95*, 13–25.
- Iwata, Y.; Koseki, H.; Hosoya, F. Study on Decomposition of Hydroxylamine/Water Solution. *J. Loss Prev. Process Ind.* **2003**, *16*, 41–53.
- Iwata, Y.; Koseki, H. Risk Evaluation of Decomposition of Hydroxylamine/Water Solution at Various Concentrations. *Process Saf. Prog.* **2002**, *21*, 136–141.
- Wei, C. Thermal Runaway Reaction Hazard and Decomposition Mechanism of the Hydroxylamine. Ph.D. Thesis, Texas A&M University, 2005.
- Wei, C.; Wang, Q.; Rogers, W. J.; Mannan, M. S.; Hall, M. B.; Pérez L. M. Thermal Decomposition Pathways of Hydroxylamine: a Theoretical Study of the Initial Steps. To be submitted for publication, 2009.
- Barton, J.; Rogers, R. *Chemical Reaction Hazards*; Institution of Chemical Engineers: Rugby, U.K., 1993.
- Fauske, H. K. The Reactive System Screening Tool (RSST): An Easy, Inexpensive Approach to the DIERS Procedure. *Process Saf. Prog.* **1998**, *17*, 190–195.

- (29) Singh, J.; Simms, C. In *Reactive Chemical Screening: a Widespread Weak Link?* Proceedings of the 2nd Annual Mary Kay O'Connor Process Safety Center Symposium – Beyond Regulatory Compliance: Making Safety Second Nature, MKOPSC: College Station, TX, October 26–27, 1999; pp 240–250.
- (30) Leung, J. C.; Fisher, H. G. In *Runaway Reaction Characterization: a Round-Robin Study on Three Additional Systems*, Proceedings AIChE DIERS - 2nd International Symposium of Runaway Reactions, Pressure Relief Design, and Effluent Handling, New Orleans, LA, March 11–13, 1998; Melhem, G. A., Fisher H. G., Eds.; AIChE N: New York, 1998; pp 109–134.
- (31) Townsend, D. I.; Tou, J. T. Thermal Hazard Evaluation by an Accelerating Rate Calorimeter. *Thermoquim. Acta* **1980**, *37*, 1–30.
- (32) Chippett, S.; Ralbovsky, P.; Granville, R. In *The APTAC: a High pressure, Low Thermal Inertia, Adiabatic Calorimeter*, Proceedings AIChE DIERS - 2nd International Symposium of Runaway Reactions, Pressure Relief Design, and Effluent Handling., New Orleans, LA, March 11–13, 1998; Melhem, G. A., Fisher H. G., Eds.; AIChE N: New York, 1998; pp 81–108.
- (33) Tamy, G.; Schreiber, L. B. In *Adiabatic Calorimetric Evaluation for Safe Process Scale-up*; Proceedings AIChE DIERS - 2nd International Symposium of Runaway Reactions, Pressure Relief Design, and Effluent Handling, New Orleans, LA, March 11–13, 1998; Melhem, G. A., Fisher H. G., Eds.; AIChE N: New York, 1998; pp 65–79.
- (34) Lewis, R. J.; Sax N. I. *Dangerous Properties of Industrial Materials*, 8th ed.; Van Nostrand Reinhold: New York, 1992.
- (35) *Standard Methods for the Examination of Water and Wastewater*, 19th ed.; Eaton, A. D., Clesceri, L. S., Greenberg, A. E., Eds.; American Public Health Association, American Water Works Association, and Water Environment Federation: WA, 1995.
- (36) *Hazard Evaluation Laboratory. SIMULAR Reaction Calorimeter, Operating Manual*; Barnet, U.K., 1998; Vols. 1–3.
- (37) Kashima, C.; Yoshiwara, N.; Omote, Y. Alkylation of Aminohydroxy Anion, Dissociated Species of Hydroxylamine. *Tetrahedron Lett.* **1982**, *23*, 2955–2956.

Received for review January 30, 2009. Accepted March 26, 2009. Part of this research was sponsored by Mary Kay O'Connor Process Safety Center, Chemical Engineering Department, Texas A&M University.

JE9001366